Chemometric Studies on Brain-uptake of PET Agents *via* VolSurf Analysis

Hyo Seon Lee, Mi Kyoung Kim, Chaewoon Lee, Jinyoung Kim, Il Han Choo,† Jong Inn Woo,† and Youhoon Chong*

*Department of Bioscience and Biotechnology, Konkuk University, Seoul 143-701, Korea. *E-mail: chongy@konkuk.ac.kr*
†Department of Neuropsychiatry, Seoul National University College of Medicine, Seoul 110-744, Korea
Received September 13, 2007

High initial (2 minutes after iv injection) brain-uptake of PET agents is required to deliver the agent to binding sites in brain tissue but, for quantification of the specific binding, relatively rapid washout of free and non-specifically bound PET agents from the brain (30 minutes after injection) also is required. In order to compare the physicochemical properties of the PET agents which are responsible for early brain-uptake and rapid washout, respectively, chemometric analysis on brain-uptake of PET agents was performed *via* a classical VolSurf approach. According to the PCA and PLS results, high 2-30 min brain-uptake ratio seems to be related to the large hydrophobic regions in the PET agents which are not confined to a particular surface.

Key Words : PET, β-Amyloid, VolSurf, Brain-uptake, Rapid washout

Introduction

Alzheimer's disease (AD) is a neurodegenerative disease of the brain associated with irreversible cognitive decline, memory impairment and behavioral changes. Currently, the only definitive confirmation of AD is by postmortem histopathological examination of senile plaques (β-amyloid, Aβ-plaques) in the brain.[1] While there are no definitive treatments available to affect a cure of AD, much recent interest has been given to the development of anti-amyloid therapies aimed at halting and reversing Aβ-deposition and, thus, monitoring of the therapeutic efficacy would greatly benefit from methods for the *in vivo* detection and quantification of Aβ-deposits in the brain.[2]

Agents for the *in vivo* imaging of Aβ-plaques with positron emission tomography (PET) or single-photon emission computed tomography (SPECT) have been reported by several research groups, which are based on highly conjugated dyes such as congo red, chrysamine G, and thioflavin T. In order to produce an image, the imaging agents should penetrate into the brain and bind to the Aβ-plaques. Thus, the brain-uptake is a critical factor in determining the effectiveness of the PET agent. There is a broad consensus that the initial brain-uptake of the radioligands can be explained by the permeability of the blood-brain barrier (BBB). Previous studies suggest that the optimal lipophilicity range for brain entry is observed for compounds with logP values between 1 and 3. Below that range, passive diffusion through the BBB is poor, and above that range, binding of any radiotracers to blood components is so great as to limit the amount available for brain entry. While high initial brain-uptake is required to deliver the agent to binding sites in brain tissue, relatively rapid washout of free and non-specifically bound radiolabel from the brain in 30 min or less also is required in order to quantify specific binding to sites of interest. Particularly for relatively short-lived ^{11}C-labeled radioligands, the rapid washout is an appropriate pharmacokinetic property for early detection of amyloid plaques in the AD brain, which was shown in the successful development of *N*-[^{11}C-methyl]-6-OH-BTA-1 ([^{11}C]PIB).[3,4] Although many factors such as molecular size, ionic charge, and lipophilicity affect the brain clearance of compounds, the precise mechanisms responsible for the rapid clearance of the PET agents from the normal brain still remain unknown.[5-7] Thus, in this study, we made the here to unknown attempt to compare the physicochemical properties of the PET agents which are responsible for early brain-uptake and rapid washout, respectively, by construction of chemometric models *via* a VolSurf approach.

Results and Discussion

Pharmacokinetic properties are often the bottleneck in drug discovery, being closely linked with partitioning, solubility and membrane transport. It is well known that the drug orientation and its rate of movement within the biological membrane are related to its size and shape. VolSurf is a computational procedure, which is specifically designed to produce descriptors related to pharmacokinetic properties such as partitioning and membrane transport starting from 3D interaction energy grid maps produced by GRID program. In this study, in order to identify the physicochemical properties responsible for efficient initial brain-uptake as well as rapid washout of PET agents, a chemometric analysis was performed by using the VolSurf approach.

PCA Analysis. In a first step, VolSurf descriptors (Table 1) were derived using the water (OH2), the lipophilic (DRY) and the hydrogen bond acceptor (O) probe, which were rearranged in a X data matrix made of 25 rows (the training set molecules, Fig. 1) and 94 column variables (the calculated variables).

Then the PCA works by decomposing the X-matrix as the product of two smaller matrices, which are called loading and score matrices. The loading matrix is composed of a few vectors (Principal Components, PCs) which are obtained as linear combinations of the original X-variables and it con-

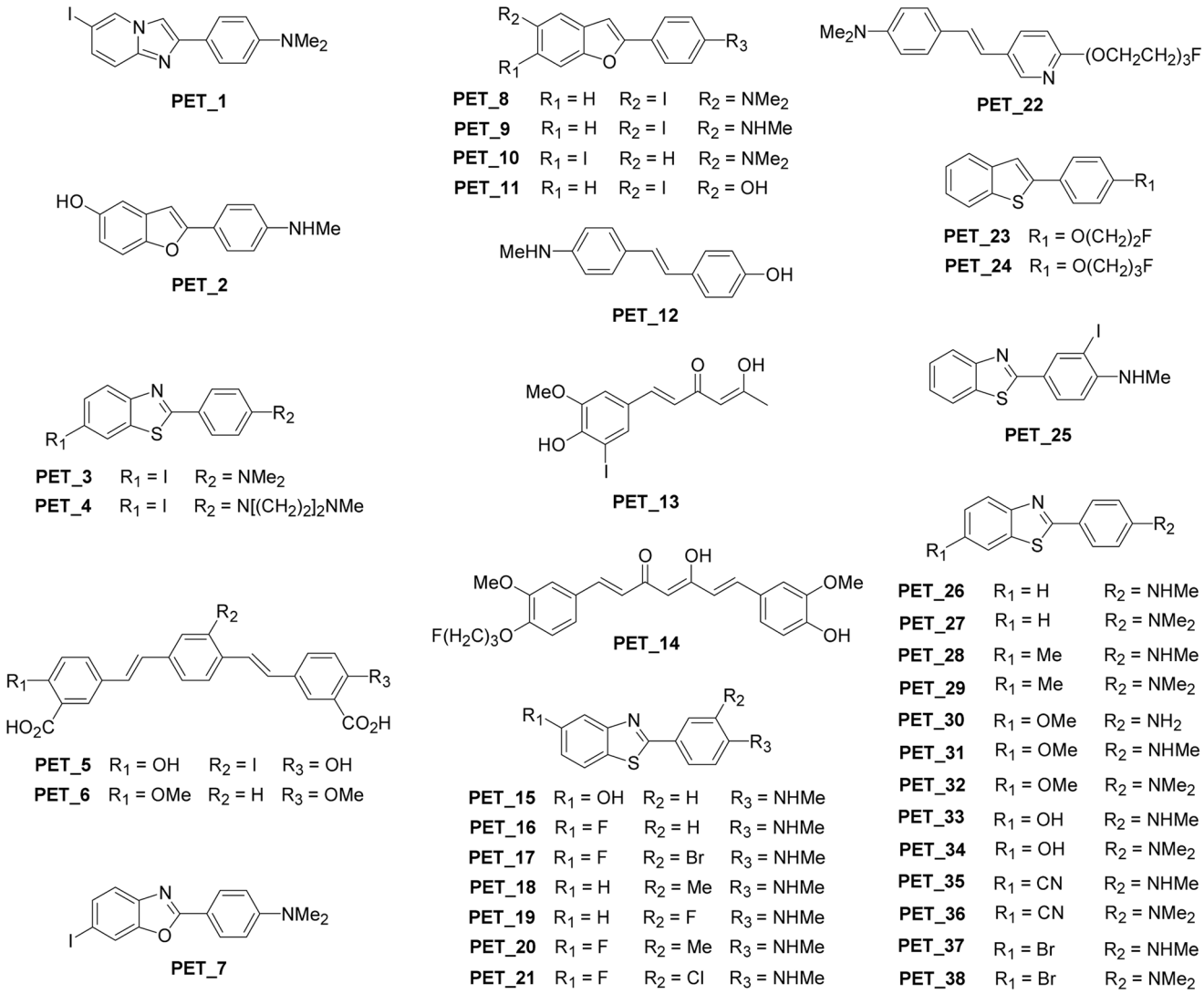

Figure 1. PET agents used for VolSurf analysis.

tains information about the variables (structural features). The score matrix contains information about the objects, and each object is described in terms of its projections onto the PCs instead of the original variables. In this study, five significant principal components were observed by cross-validation technique (Table 2), which explained about 78% of the total variance of the matrix, the first two PCs being most informative.

The best way to extract information from the PCA is through a few informative diagrams (score plot and loading plot) which permit a simple, straightforward interpretation of the problem under investigation. Figures 2 and 3 show the score plot of the second versus the first component and the corresponding loading plot, respectively. The score plots were color coded according to their 2-min (Fig. 2a) and 30-min (Fig. 2b) brain-uptake values (Table 3) with most active compounds colored red triangle followed by orange circle, pink rectangle, green diamond and then blue bar for the least potent compounds. Clearly, all top 10 compounds (red triangles and orange dots) are observed to lie in the same cluster which is marked by an ellipse in the score plot color coded by 2-min brain-uptake values (Fig. 2a) whereas no clustering could be identified on the basis of the 30-min data (Fig. 2b).

As the PCA analysis does not require external information (activity data) or training, the score plot which shows that the generated VolSurf descriptors restricted the most active compounds to a specific region (Fig. 2a) can be used as a projection map to understand the early brain-uptake properties of the untested PET agents. On the other hand, as the score plot fails to cluster the PET agents according to the 30-min brain-uptake data, rapid washout property of PET agents cannot be properly projected by the PCA analysis.

Turning our attention to the loading plot (Fig. 3), the loading of a single variable indicates how much this variable participates in defining the PC. Variables contributing very little to the PCs have small loading values and are plotted around the center of the plot. On the other hand the variables that contribute most are plotted around the borders of the plot. In the loading plot of the PET agents (Fig. 3), the

Table 1. Used descriptors for calculation by VolSurf program

No	Code	Probes			Description
		OH2	DRY	O	
1	V	O			Molecular Volume
2	S	O			Molecular Surface
3	R	O			Volume/surface ratio
4	G	O			Molecular Globularity
5-12	W1-W8	O			Hydrophilic Regions
13-18	BV11-BV32	O			Hydrophilic Best Volumes
19-26	Iw1-Iw8	O			Integy Moment
27-34	Cw1-Cw8	O			Capacity Factor
35-37	Emin1-Emin3	O			Hydrophilic Local Interaction Energy Minima
38-40	D12-D23	O			Hydrophilic Local Interaction Energy Minima Distances
41-48	D1-D8		O		Hydrophobic Regions
49-54	BV11-BV32		O		Hydrophobic Best Volumes
55-62	ID1-ID8		O		Hydrophobic Integy Moments
63-65	Emin1-Emin3		O		Hydrophobic Local Interaction Energy Minima
66-68	D12-D23		O		Hydrophobic Local Interaction Energy Minima Distances
69-70	HL1-HL2				Hydrophilic-Lipophilic Balance
71	A				Amphiphilic Moment
72	CP				Critical Packing
73-80	W1-W8			O	Hydrophilic Regions
81-88	HB1-HB8			O	Hydrogen Bonding
89	POL				Polarizability
90	MW				Molecular Weight
91	Elon				Elongation
92	EEFR				Elongation
93	DIFF				Diffusivity
94	LogP				LogP

Table 2. Summary of PCA analysis

Components	XVarExp	XAccum
1	36.11	36.11
2	15.99	52.10
3	13.32	65.42
4	8.20	73.62
5	4.12	77.74

XVarExp: Percentage of X-matrix variance explained by the corresponding component. XAccum: Accumulative percentage of the X-matrix variance explained by the model

VolSurf descriptors that are contributing most in PC1, explaining major portion of the PC2, and contributing very little to the PCs are encircled blue box, red circle and black ellipse, respectively.

The first PC (PC1, x-axis, Fig. 3) mainly classifies molecules according to the distribution of hydrophilic regions around them. Molecules with negative scores are influenced most by integy moments Iw4-Iw6 and by diffusivity DIFF. Integy moments measure the imbalance between the center of mass of a molecule and the position of hydrophilic or hydrophobic regions around it. If the integy moment is high, there is a clear concentration of hydrated or hydrophobic regions in only one part of the molecular surface. If the integy moment is small, the polar or hydrophobic moieties

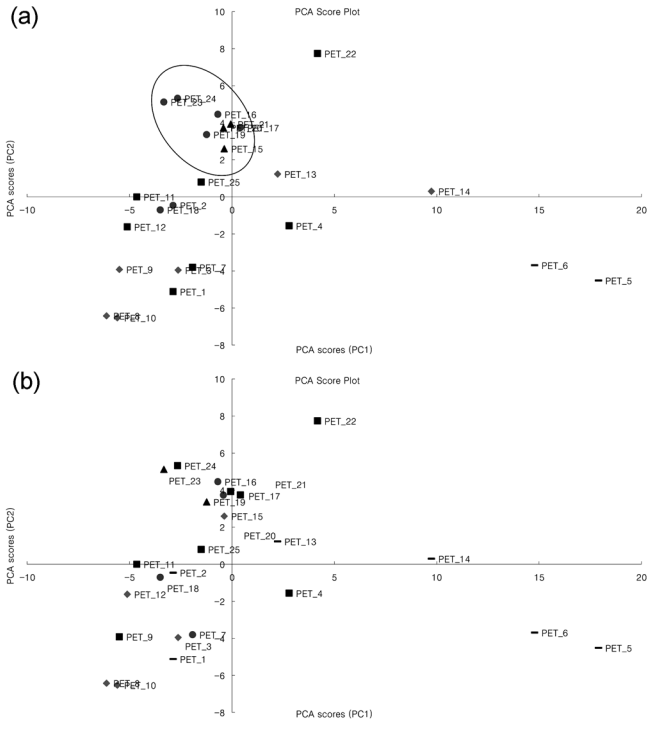

Figure 2. Score plot of PC1 versus PC2 for PCA model. Compounds are colored according to (a) 2-min brain-uptake values and (b) 30-min brain-uptake values.

Table 3. Brain-uptake of PET agents measured in mice at 2 and 30 min after iv injection

Comp	brain-uptake −log (% ID/g)[a]		Comp	brain-uptake −log (% ID/g)[a]		Comp	brain-uptake −log (% ID/g)[a]	
	2 min	30 min		2 min	30 min		2 min	30 min
PET_1	–0.46	0.59	**PET_14**	0.28	0.96	**PET_27**	0.72[c]	1.11[c]
PET_2	–0.68	0.46	**PET_15**	–1.01	0.02[b]	**PET_28**	0.66[c]	1.08[c]
PET_3	0.22	0.05	**PET_16**	–0.79	–0.39[b]	**PET_29**	1.11[c]	0.82[c]
PET_4	–0.18	–0.20	**PET_17**	–0.61	–0.21[b]	**PET_30**	0.49[c]	1.08[c]
PET_5	0.57	1.22	**PET_18**	–0.75	–0.30[b]	**PET_31**	0.32[c]	0.00[c]
PET_6	0.85	1.52	**PET_19**	–0.99	–0.50[b]	**PET_32**	0.10[c]	0.07[c]
PET_7	–0.16	–0.32	**PET_20**	–1.10	–0.30[b]	**PET_33**	0.31[c]	–0.24[c]
PET_8	0.29	0.05	**PET_21**	–1.29	–0.29[b]	**PET_34**	0.31[c]	0.00[c]
PET_9	0.11	–0.08	**PET_22**	–0.48	–0.12	**PET_35**	0.31[c]	–0.08[c]
PET_10	0.32	0.10	**PET_23**	–0.54	–0.58	**PET_36**	0.21[c]	0.00[c]
PET_11	–0.15	–0.26	**PET_24**	–0.52	–0.15	**PET_37**	0.04[c]	0.04[c]
PET_12	–0.06	0.38	**PET_25**	–0.32	–0.20	**PET_38**	–0.10[c]	0.02[c]
PET_13	0.16	0.96	**PET_26**	0.37[c]	1.24[c]			

[a]Percent injected dose per gram. [b]Recalculated from 2-30 min uptake ratio. [c]Brain-uptake data are normalized to body weight (in kg). Thus, the data are expressed in (%ID-kg)/g

are either close to the center of mass or they are at opposite ends of the molecule. At the positive extremity, the first PC is influenced most by capacity factors Cw, hydrophilic best volume BV, and hydrophilic regions W, which define the amount of hydrophilic regions per surface unit, the best three hydrophilic volumes generated by a water molecule when interacting with the target, and the molecular envelope accessible to the solvent water molecule, respectively. Thus, the molecules characterized by negative PC1 scores show a localized hydrophobic region, while molecules with positive PC1 scores show hydrophilic regions distributed over greater surface areas, and the hydrophobic regions do not seem to be relevant.

On the other hand, the second PC (PC2, y-axis, Fig. 3) in the negative scores region is influenced most by hydrophobic regions D1-D8 and hydrophobic best volumes BV11-BV12, which define interaction with DRY probe and the best three hydrophobic volumes generated by a DRY probe when interacting with the target, respectively. In the positive score value region the second PC is determined most by hydrophobic integy moments ID1-ID8. Taken together, the molecules characterized by negative PC2 scores show hydrophobic regions distributed over greater surface areas, while molecules with positive PC2 scores show localized hydrophobic regions.

It is worth to note that the top 10 active PET agents are

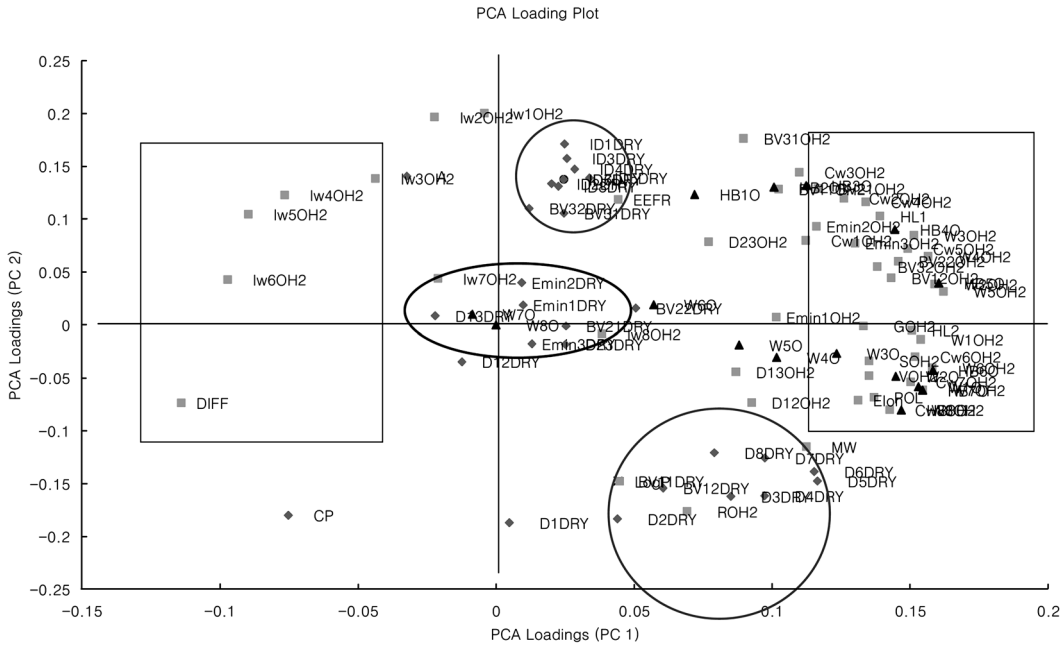

Figure 3. Loading plot of PC1 versus PC2 for PCA model.

located along the positive y-axis of the score plot (Fig. 2a), and thus, it can be hypothesized that for PET agents to have good brain-uptake 2 minutes after intravenous injection, they should be characterized by a localized hydrophobic region. The information obtained is of particular interest since PCA, which does not explicitly consider the activity of the considered structures nor training was explicitly made, was able to divide the molecules in such a way that the biological activity was recognized in a correct ranking order around the series of compounds.

PLS Analysis. As a next part of our work, like in other QSAR methods, we tried to predict the biological activities by using PLS analysis. PLS has been shown to be one of the

Table 4. Summary of PLS analysis

	Brain-uptake after 2 min	Brain-uptake after 30 min
q^2	0.749	0.616
r^2	0.950	0.806
N	5	2
SDEP	0.272	0.339
SDEC	0.121	0.241
% of Variance	73.219	49.518

q^2: Cross-validated correlation coefficient. *N*: Optimum number of components. r^2: Non-cross-validated correlation coefficient. SDEP: Standard deviation of error of predictions. SDEC: Standard deviation of error of calculations

Table 5. Experimental versus calculated brain-uptake values of training set and test set of the PET agents obtained from PLS analysis

(a) Training set

Comp	brain-uptake, 2 min –log (% ID/g)[a]			Comp	brain-uptake, 30 min –log (% ID/g)[a]		
	Exp[b]	Calc[b]	Res[b]		Exp	Calc	Res
PET_1	–0.46	–0.27	–0.19	**PET_1**	0.59	0.22	0.37
PET_2	–0.68	–0.61	–0.07	**PET_2**	0.46	0.17	0.29
PET_3	0.22	0.07	0.16	**PET_3**	0.05	0.07	–0.02
PET_4	–0.18	–0.14	–0.04	**PET_4**	–0.20	0.15	–0.35
PET_5	0.57	0.55	0.02	**PET_5**	1.22	1.49	–0.27
PET_6	0.85	0.81	0.05	**PET_6**	1.52	1.41	0.11
PET_7	–0.16	–0.14	–0.01	**PET_7**	–0.32	0.22	–0.54
PET_8	0.29	0.38	–0.09	**PET_8**	0.05	0.16	–0.12
PET_9	0.11	0.06	0.04	**PET_9**	–0.08	0.08	–0.16
PET_10	0.32	0.20	0.11	**PET_10**	0.10	0.18	–0.08
PET_11	–0.15	–0.10	–0.05	**PET_11**	–0.26	0.04	–0.30
PET_12	–0.06	–0.31	0.25	**PET_12**	0.38	0.19	0.18
PET_13	0.16	0.19	–0.03	**PET_13**	0.96	0.44	0.52
PET_14	0.28	0.40	–0.12	**PET_14**	0.96	0.68	0.28
PET_15	–1.01	–0.98	–0.03	**PET_15**	0.02	–0.10	0.12
PET_16	–0.79	–1.08	0.29	**PET_16**	–0.39	–0.32	–0.07
PET_17	–0.61	–0.76	0.15	**PET_17**	–0.21	–0.26	0.05
PET_18	–0.75	–0.60	–0.15	**PET_18**	–0.30	–0.20	–0.10
PET_19	–0.99	–0.96	–0.02	**PET_19**	–0.50	–0.32	–0.18
PET_20	–1.10	–1.06	–0.03	**PET_20**	–0.30	–0.28	–0.01
PET_21	–1.29	–1.11	–0.18	**PET_21**	–0.29	–0.30	0.01
PET_22	–0.48	–0.55	0.07	**PET_22**	–0.12	–0.10	–0.03
PET_23	–0.54	–0.49	–0.06	**PET_23**	–0.58	–0.55	–0.03
PET_24	–0.52	–0.38	–0.13	**PET_24**	–0.15	–0.53	0.38
PET_25	–0.32	–0.38	0.06	**PET_25**	–0.20	–0.15	–0.05

(b) Test set

Comp	2-30 min ratio of brain-uptake[c]			Comp	2-30 min ratio of brain-uptake		
	Exp	Calc	Res		Exp	Calc	Res
PET_26	–0.88	–0.36	–0.52	**PET_33**	–1.07	–0.69	–0.38
PET_27	–0.39	–0.21	–0.18	**PET_34**	–0.51	–0.53	0.02
PET_28	–0.42	–0.32	–0.10	**PET_35**	–0.71	–0.59	–0.12
PET_29	–0.28	–0.15	–0.13	**PET_36**	–0.39	–0.44	0.05
PET_30	–0.58	–0.63	0.05	**PET_37**	0.00	–0.28	0.28
PET_31	–0.52	–0.44	–0.08	**PET_38**	0.31	–0.13	0.44
PET_32	–0.06	–0.31	0.25				

[a]Percent injected dose per gram. [b]Exp: Experimental, Calc: Calculated, Res: Residual. [c]Ratio between the early brain-uptake vale and persistent brain-uptake value

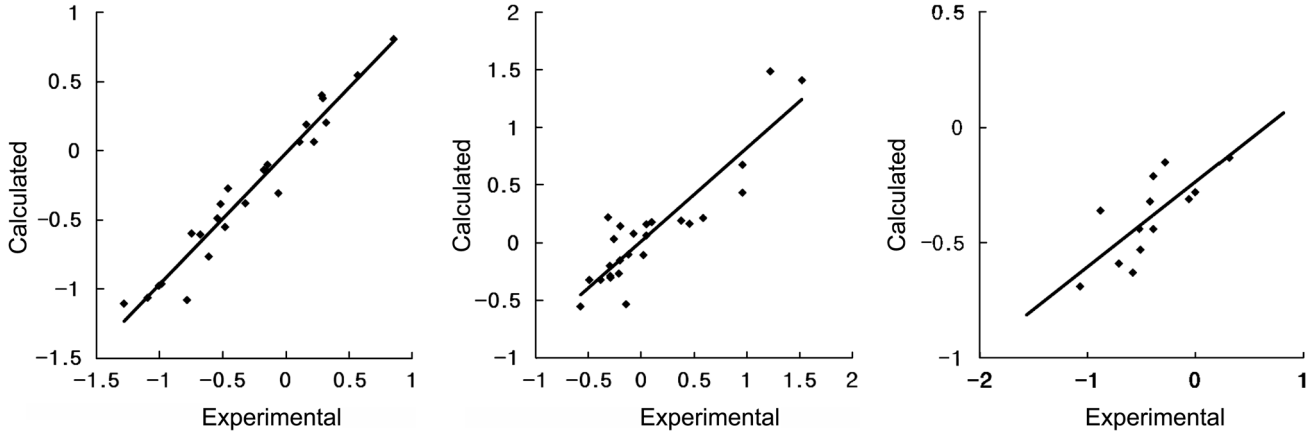

Figure 4. (a) Plot of experimental versus calculated brain-uptake values of PET agents 2 min after iv injection. (b) Plot of experimental versus calculated brain-uptake values of PET agents 30 min after iv injection. (c) Plot of experimental versus calculated 2-30 min brain-uptake ratio values of PET agents.

most appropriate regression methods to derive QSAR models. The objective of the analysis is to provide a relationship between the Y-vector (biological activity data) and the X-matrix so that the biological behavior of a series of molecules can be explained. A PLS model describes the X-matrix by a PC-like model and the Y-vector as a predictive relationship with the PCs. The analysis on the 2-min brain-uptake data led to a five-component model with leave-one-out (LOO) cross-validated r^2 (q^2) value of 0.749 and conventional r^2 of 0.950 explaining 73% of the variance of the data (Table 4). In case of 30-min brain-uptake data a model of two components with cross-validated r^2 (q^2) value of 0.616 and conventional r^2 of 0.806 which explains 50% of the total variance of the data was obtained (Table 4).

Both models were used to predict the activities of the external training set containing 13 compounds (Table 5), and Figure 4 shows the results obtained in terms of experimental versus recalculated values for the 2-min model, 30-min model and test set. As the literature for the test set molecules presents brain-uptake data normalized to the mouse body weight [(%ID-kg)/g], direct comparison of the experimental data with the recalculated data obtained from the model trained by (%ID/g) data is not feasible, and thus, 2-30 min ratio of brain-uptake was used to evaluate the predictive ability of the model, which provided fair prediction for all the compounds with residual values less than one log unit (Table 5).

The VolSurf descriptors with the strongest impact on brain-uptake of PET agents are highlighted in PLS coefficient plots in Figure 5. Brain-uptake 2 minutes after intravenous injection particularly increases with high values of the volume/surface ratio of the water probe (ROH), hydrophobic regions (D) and best volumes (BV) of the DRY probe, and molecular weight (MW) (Fig. 5a). Conversely integy moments of the water probe (Iw) is inversely related to the brain-uptake (Fig. 5a). Taken together, for efficient initial brain-uptake of PET agents, hydrophobic regions are optimal but hydrophilic regions strictly confined to a particular surface are detrimental. The hydrophobic regions (D) and best volumes (BV) of the DRY probe also plays the key role in taking the PET agents inside the brain 30 minutes after injection, but several other factors such as high values of the hydrophilic best volume (BV) and the hydrophilic local interaction minima (D) of the water probe, hydrophobic integy moments (ID) and hydrophobic local interaction energy minima (Emin) of the DRY probe, and hydrophilic regions (W) of the hydrogen bond acceptor probe exert significant impact on brain-uptake of the ligands (Fig. 5b). For clear comparison of the descriptors which are important for initial brain-uptake (2-min data, Fig. 5a) and rapid washout (30-min data, Fig. 5b), relative changes of the PLS coefficients of 94 VolSurf descriptors were calculated which is shown in Figure 5c. Thus, high positive values of the relative changes indicate significant decrease of the PLS coefficients in 30-min data and negative relative changes reflect the corresponding descriptors are less important in 30-min brain-uptake. Many descriptors showed relative changes larger than 2.5 but, among them, only one descriptor [hydrophobic integy moments (ID) of the DRY probe] had the absolute coefficient larger than 20% of the maximum value (Fig. 5c), which could give significant impact on brain-uptake of PET agents. This result clearly shows that high ID of the DRY probe is the major descriptor for characterization of the PET agents which can be rapidly taken up by the brain (high 2-min brain-uptake values) and kept inside the brain 30 minutes after injection (high 30-min brain-uptake values). In other words, among compounds which have good initial brain-uptake values, particularly those with concentrated regions of hydrophobicity would have a strong tendency to stay for a long time in the brain, which is an inappropriate property for a good PET agent. Thus, the concentrated hydrophobicity seems to help initial brain-uptake of the PET agents but it has a detrimental effect on the escape of the molecule from the brain to result in high brain concentration after 30 minutes.

In conclusion, taking the results of the chemometric study (PCA and PLS analyses) together, we can propose physicochemical properties of PET agents for high initial brain-

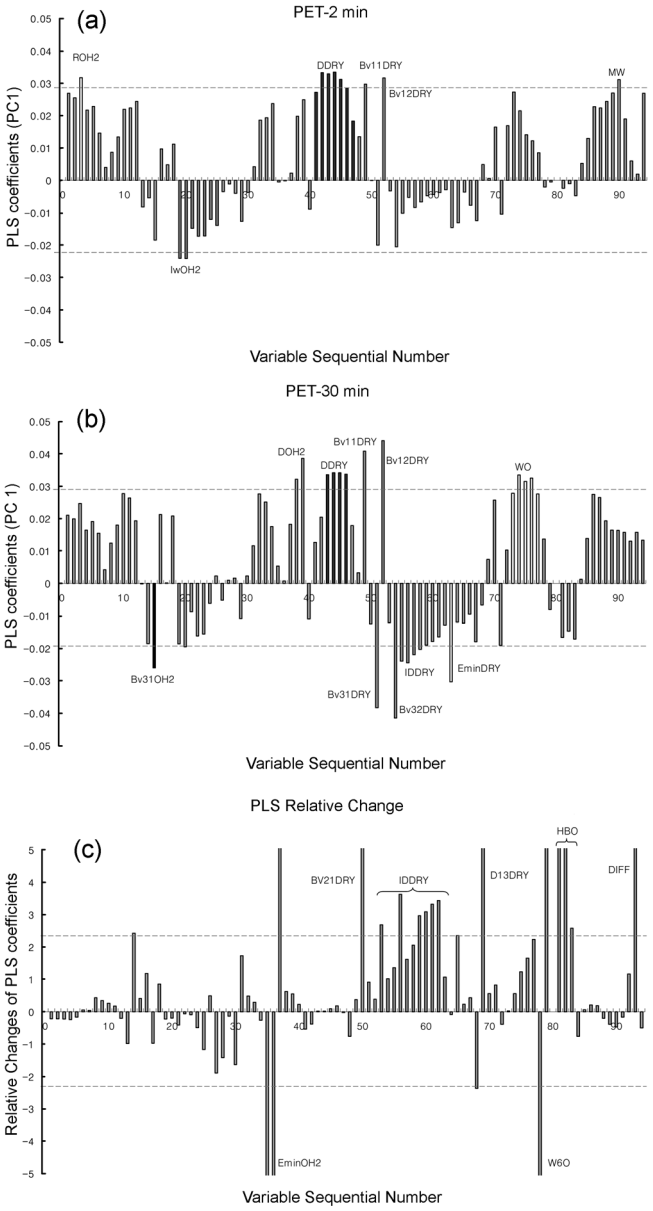

Figure 5. PLS coefficients plot for the correlation of VolSurf descriptors with brain-uptake. (a) Plot for 2-min brain-uptake. (b) Plot for 30-min brain-uptake. (c) Relative change in brain-uptake between 2-min and 30-min data.

uptake but rapid washout. High early brain-uptake seems to be related to the large and concentrated hydrophobic regions but for rapid washout the hydrophobic region should not be confined to a particular surface. Thus, this study indicates that the hydrophobic integy moments (ID) play the key role in determining the efficiency of the PET agents, which provides valuable insights in developing novel PET agents.

Experimental Section

Databases. The training set comprises 25 PET agents (**PET_1**~**PET_25**, Fig. 1) which were reported with initial brain-uptake values along with washout data in the literature.[8] The test set includes 6-substituted 2-arylbenzothiazoles (**PET_26** ~ **PET_38**, Fig. 1) of which brain-uptake data are normalized to mouse body weight (in kg) and thus, direct comparison with other literature data is not possible.[9]

3D-Structures Generation. Molecular models and geometry optimizations were performed using the software package SYBYL v 7.2 running on a Linux workstation under the enterprise operating system. All compounds were constructed by the Sketch module in SYBYL base, assigned with MMFF94s charges and minimized with MMFF94s[10] force field. Conformational analysis was not performed because the structures used have only one rotatable bond bridging two aryl groups of which rotation does not produce energetically different conformations. Also, VolSurf descriptors are known to be relatively independent of the conformation of molecules.[11,12]

Chemical Descriptors. VolSurf Descriptors. VolSurf is a computational procedure to produce 2D molecular descriptors from 3D molecular interaction energy grid maps.[11,12] The basic idea of VolSurf is to compress the information present in 3D maps into a few 2D numerical descriptors which are very simple to understand and to interpret. The molecular descriptors were derived by using the VolSurf/GRID program, which is a computational procedure for producing and exploring the physicochemical property space of a molecule, starting from 3D interaction energies grid maps between the target molecule and different chemical probes. In our study we used the probes water (OH2), hydrophobic (DRY) and H-bonding carbonyl (O) to generate the 3D interaction energies and a Grid space of 0.5 Å. As a result, VolSurf generated 94 physicochemical descriptors reported in Table 1.

Statistical Analysis. Complexity reduction and data simplification are two of the most important features of the VolSurf package which includes chemometric tools such as principal component analysis (PCA) and partial least squares analysis (PLS) for extracting and rationalizing the information from any multivariate description of a biological system. Two PCA diagrams (score plot and loading plot) were plotted in the space of the principal components (PCs). PLS regression technique was used to derive a QSAR model of the PET agents. The predictive ability of the generated PLS model was evaluated using leave-one-out (LOO) cross-validation. External prediction set (test set) was also used to evaluate the predictive ability of the model. Thus, the original data set are split up into two groups from the very beginning of the analysis. The first one, the training set, was used to build the PLS model and the other, the test set, was used to compare the experimental Y-values with the predictions made by the model.

Acknowledgments. This work was supported by grant KRF-2007-313-C00476 from the Korea Research Foundation, Republic of Korea (MOEHRD, by a grant (20050301-034-449-112-02-00) from BioGreen 21 Program, Rural Development Administration, Republic of Korea, and the second Brain Korea 21 (Korea Ministry of Education). HSL, MKK and JK are supported by the second Brain Korea 21.

References

1. (a) Hardy, J.; Selkoe, D. J. *Science* **2002**, *297*, 353. (b) Lim, H.-J.; Jung, M. H.; Lee, I. Y. C.; Park, W. K. *Bull. Korean Chem. Soc.* **2006**, *27*, 1371. (c) Kim, J.; Myung, E.-K.; Lee, I.-H.; Paik, W. K. *Bull. Korean Chem. Soc.* **2007**, *28*, 2283.
2. Nordberg, A. *Lancet Neurol.* **2004**, *3*, 519.
3. Klunk, W. E.; Engler, H.; Nordberg, A.; Wang, Y.; Blomqvist, G.; Holt, D. P.; Bergstrom, M.; Savitcheva, I.; Huang, G. F.; Estrada, S.; Ausen, B.; Debnath, M. L.; Barletta, J.; Price, J. C.; Sandell, J.; Lopresti, B. J.; Wall, A.; Koivisto, P.; Antoni, G.; Mathis, C. A.; Langstrom, B. *Ann. Neurol.* **2004**, *55*, 306.
4. Price, J. C.; Klunk, W. E.; Lopresti, B. J.; Lu, X.; Hoge, J. A.; Ziolko, S. K.; Holt, D. P.; Meltzer, C. C.; Dekosky, S. T.; Mathis, C. A. *J. Cereb. Blood Flow Metab.* **2005**, *25*, 1528.
5. Dishino, D. D.; Welch, M. J.; Kilbourn, M. R.; Raichle, M. E. *J. Nucl. Med.* **1983**, *24*, 1030.
6. Levin, V. A. *J. Med. Chem.* **1980**, *23*, 682.
7. Feher, M.; Sourial, E.; Schmidt, J. M. *Int. J. Pharm.* **2000**, *201*, 239.
8. (a) Cai, L.; Chin, F. T.; Pike, V. W.; Toyama, H.; Liow, J.-S.; Zoghbi, S. S.; Modell, K.; Briard, E.; Shetty, H. U.; Sinclair, K.; Donohue, S.; Tipre, D.; Kung, M.-P.; Dagostin, C.; Widdowson, D. A.; Green, M.; Gao, W.; Herman, M. M.; Ichise, M.; Innis, R. B. *J. Med. Chem.* **2004**, *47*, 2208. (b) Ono, M.; Kawashima, H.; Nonaka, A.; Kawai, T.; Haratake, M.; Mori, H.; Kung, M.-P.; Kung, H. F.; Saji, H.; Nakayama, M. *J. Med. Chem.* **2006**, *49*, 2725. (c) Zhuang, Z.-P.; Kung, M.-P.; Wilson, A.; Lee, C.-W.; Plössl, K.; Hou, C.; Holtzman, D. M.; Kung, H. F. *J. Med. Chem.* **2003**, *46*, 237. (d) Zhuang, Z.-P.; Kung, M.-P.; Hou, C.; Plössl, K.; Skovronsky, D.; Gur, T. L.; Trojanowski, J. Q.; Lee, V. M.-Y.; Kung, H. F. *Nucl. Med. Biol.* **2001**, *28*, 887. (e) Ono, M.; Kung, M.-P.; Hou, C.; Kung, H. F. *Nucl. Med. Biol.* **2002**, *29*, 633. (f) Ono, M.; Wilson, A.; Nobrega, J.; Westaway, D.; Verhoeff, P.; Zhuang, Z.-P.; Kung, M.-P.; Kung, H. F. *Nucl. Med. Biol.* **2003**, *30*, 565. (g) Henriksen, G.; Hauser, A.; Westwell, A. D.; Yousefi, B. H.; Schwaiger, M.; Drzezga, A.; Wester, H.-J. *J. Med. Chem.* **2007**, *50*, 1087. (h) Chang, Y. S.; Jeong, J. M.; Lee, Y.-S.; Kim, H. W.; Rai, B. G.; Kim, Y. J.; Lee, D. S.; Chung, J.-K.; Lee, M. C. *Nucl. Med. Biol.* **2006**, *33*, 811. (i) Zhuang, Z.-P.; Kung, M.-P.; Hou, C.; Skovronsky, D. M.; Gur, T. L.; Plössl, K.; Trojanowski, J. Q.; Lee, V. M.-Y.; Kung, H. F. *J. Med. Chem.* **2001**, *44*, 1905. (j) Ryu, E. K.; Choe, Y. S.; Lee, K.-H.; Choi, Y.; Kim, B.-T. *J. Med. Chem.* **2006**, *49*, 6111. (k) Chandra, R.; Kung, M.-P.; Kung, H. F. *Bioorg. Med. Chem. Lett.* **2006**, *16*, 1350.
9. Mathis, C. A.; Wang, Y.; Holt, D. P.; Huang, G.-F.; Debnath, M. L.; Klunk, W. E. *J. Med. Chem.* **2003**, *46*, 2740.
10. (a) Halgren, T. A.; Nachbar, R. B. *J. Comput. Chem.* **1996**, *17*, 587. (b) Halgren, T. A. *J. Comput. Chem.* **1999**, *20*, 730.
11. Cruciani, G.; Crivori, P.; Carrupt, P.-A.; Testa, B. *J. Mol. Struct. (THEOCHEM)* **2000**, *503*, 17.
12. Crivori, P.; Cruciani, G.; Carrupt, P.-A.; Testa, B. *J. Med. Chem.* **2000**, *43*, 2204.